History effect in inhomogeneous superconductors

Y. Liu, H. Luo, X. Leng, Z. H. Wang, L. Qiu, and S. Y. Ding*
Department of Physics and National Laboratory of Solid State Microstructures, Nanjing University, Nanjing 210093, People's Republic of China

L. Z. Lin
Institute of Electric Engineering, Chinese Academy of Science, Beijing 100080, People's Republic of China
(Received 19 September 2001; revised manuscript received 28 January 2002; published 29 October 2002)

A model was proposed to account for a different kind of history effect in the transport measurement of a sample with inhomogeneous flux pinning coupled with flux creep. The inhomogeneity of flux pinning was described in terms of alternating weak pinning (lower j_c) and strong pinning regions (higher j_c). The flux creep was characterized by logarithmic barrier. Based on this model, we numerically observed the same clockwise *V-I* loops as reported in references. Moreover, we predicted behaviors of the *V-I* loop at different sweeping rates of applied current dI/dt and magnetic fields B_a, etc. Electric transport measurement was performed in Ag-sheathed $Bi_{2-x}Pb_xSr_2Ca_2Cu_3O_y$ tapes immersed in liquid nitrogen with and without magnetic fields. A *V-I* loop at certain dI/dt and B_a was observed. It is found that the area of the loop is more sensitive to dI/dt than to B_a, which agrees well with our numerical results.

DOI: 10.1103/PhysRevB.66.144510 PACS number(s): 74.60.Ge, 74.72.Bk

I. INTRODUCTION

Recently the so-called history effect (HE) of vortex matter has been frequently observed by a variety of methods such as electric transport measurement, dc magnetization hysteresis, ac susceptibility, and torque techniques, and has drawn much more attention.[1–10] HE refers to that critical current density j_c of a superconductor has different values at a same field (or temperature) for either thermal, magnetic, or current cycles. The earlier observed hysteresis of *R-T* curves in the thermal cycle in fact is a kind of HE caused by first-order phase transition of vortex matter (melting or freezing).[11] Different mechanisms have been proposed to account for HE.[1–10] And a typical explanation contains two assumptions: relatively weak flux pinning and uniform small quenched disorders. Then HE is explained with a theory of disorder-order transition of vortex matter. The disordered vortex matter pinned more strongly (higher j_c) is supercooled to low temperature where it is in a metastable state and then a process such as a bias current anneals the metastable disordered state into an ordered and stable one with lower j_c. An important point is that flux creep in the models is omitted for the low temperatures. In this case, the property of vortex matter is governed only by the competition between interactions of vortices-vortices and vortices-quenched disorders.

However, a different kind of HE has been observed.[12] The hysteresis loop of *V-I* curve of polycrystalline $Bi_{2-x}Pb_xSr_2Ca_2Cu_3O_y$ (Bi2223) at liquid-nitrogen temperature was measured there (see also Fig. 6 in this paper). It is clear that such a *V-I* loop is a different kind of HE and very different from the *V-I* loop in low-temperature superconductors reported before.[1] The difference between these two kinds of HE is that the direction of the *V-I* loop is anticlockwise in Ref. 1 while clockwise in Ref. 12 and this paper. Despite that the anticlockwise loop has been explained very well, the clockwise one interested us very much.

Note that this kind of HE takes place in a system different from those with uniform and weak quenched disorders at low temperatures. First, at higher temperatures, such as liquid-nitrogen temperatures, thermal fluctuation should be important and flux creep could influence the property of vortex matter apparently.[13] In fact the influence of flux creep on the *V-I* curve and transport property of Bi2223 have been confirmed by earlier experimental and numerical results.[14–18] Second, the quenched disorders or flux pinnings are inhomogeneous in polycrystalline high-temperature superconductors (HTS's). There are weak links and grains in sintered samples such as polycrystalline Bi2223. And the flux pinning strength of the weak links at grain boundaries is very different from that of the grains.[19] In view of these two points, any models concerning the system with homogenous quenched disorders without flux creep could not be used to understand this interesting hysteresis behavior in the *V-I* curve.

A theoretical model describing irreversible electric-magnetic behaviors of a system with inhomogeneous quenched disorders has already been proposed.[20] Unfortunately, flux creep was omitted there. Moreover, this model has not been used to explain any HE, including the clockwise *V-I* loop. Experimentally, A. M. Campbell's group did many important works on inhomogeneous superconductors. They did observe the hysteresis *V-I* curves before, however, only a qualitative explanation was given. And what interests us now is how to simulate the clockwise *V-I* loop.

Considering flux creep and inhomogeneous flux pinning, we proposed a model to explain this different kind of HE. We carried out numerical simulation with this model. Upon explaining the clockwise loop of the *V-I* curve reported in Ref. 12, we further predicted some interesting phenomena. To test the predictions, electric transport measurement was conducted for a characteristic *V-I* curve of silver-sheathed $Bi_{2-x}Pb_xSr_2Ca_2Cu_3O_y$ tapes (Ag-Bi2223) immersed in liquid nitrogen with or without applied fields B_a. The clockwise loop of the *V-I* curve at certain dI/dt and B_a was

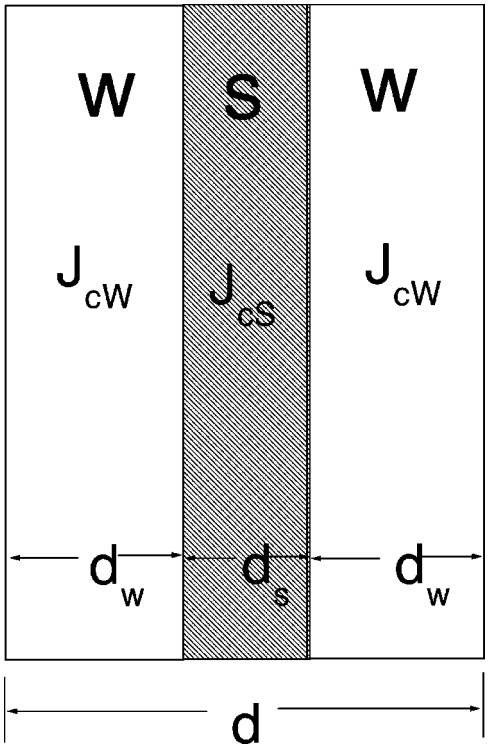

FIG. 1. A schematic sketch of the one-dimensional model: a superconducting slab consisting of periodic strong (*S*) and weak (*W*) pinning regions. Vortex lines enter the system first from the surfaces into the *W* region, and then diffuse from the *W* into the *S* regions, so the *W* region surrounds the *S* region.

observed and is dependent on dI/dt and B_a, confirming the numerical result.

II. MODEL

The model consists of two basic assumptions: there exists flux creep in a sample and the flux pinning is inhomogeneous. The complex inhomogeneity of flux pinning is simplified by a periodic strong pinning region (*S*) with large j_c (j_{cS}) and a weak pinning region (*W*) with small j_c (j_{cW}); see Fig. 1. The flux diffusion is characterized by collective creep of vortex glass, which has been discussed widely.[21] To simplify the calculation, we use a logarithmic $U(j)$ relationship, which is the special case of the vortex glass model with very small glass exponent μ.[22]

We should emphasize that our model is not a simplified version of the ''brick wall'' model, which has been widely discussed before.[23] There are some resemblances between them. However, there are at least two points that distinguish our model from the previous one. First, the brick wall model is a static critical state model without flux creep. Obviously, in any static models, the transport properties studied here will be independent of the sweeping rate of applied current dI/dt, contrasting with the experimental observation. Second, in the brick wall model the *S* and *W* regions are connected in series along the direction of current, while in our model, they are connected in parallel.

In our one-dimensional model, flux lines first enter the system from the surfaces into the weak pinning channel (*W*) and then diffuse into the strong pinning region (*S*), so *W* surrounds *S*. In other words, *S* is inside the slablike sample.

As an example, the model may be proper to polycrystalline samples of HTS's, such as silver-sheathed $Bi_{2-x}Pb_xSr_2Ca_2Cu_3O_y$ (Ag-Bi2223). The grain boundaries in polycrystalline HTS's form a weak link network of flux pinning and thus can be considered as *W*, whereas the intragrain region is *S*. It is well known that the weak link network suppresses substantially the critical current density of HTS's such as Ag-Bi2223. When current or magnetic field is applied, flux density will enter intergrain (*W*) at first and then penetrate gradually into the intragrain (*S*) by means of flux creep. Another example that the model may be applicable to is the low-temperature superconductors, such as Nb_3Sn metallic compounds, where flux lines may be pinned by a grain boundary (*S*) whereas the intragrain is a weaker pinning region (*W*).[24]

Certainly, one cannot expect that numerical results by such a simplified phenomenological model can quantitatively represent experimental data of a sample. For example, the one-dimensional geometry assumption in the model is not fulfilled for a real sample. And, the flux pinning is more complex by far than the two model parameters j_{cS} and j_{cW}. Nevertheless, our model accounts for the experimental clockwise *V-I* loop, which was observed very recently. The effectiveness of this model was demonstrated by the electric transport measurement of the hysteresis *V-I* loop.

III. SIMULATION

A. Basic equation

Consider a slab with infinite length along the *y* axis, thickness *d* along the *x* axis, and width *w* along the *z* axis. The current is applied along the *y* axis. In view of $w \gg d$, we focus on the one-dimensional case for simplicity. The nonlinear diffusion equation describing the macroscopic *B* or *j* is well known.[25,26] With a logarithmic dependence of *U* on *j*: $U(j)=U_0\ln|j_c/j|$, the diffusion equation of flux can be written as

$$\frac{\partial B}{\partial t}=\frac{v_0}{(\mu_0 j_c)^{n+1}}\frac{\partial}{\partial x}\left[\left|\frac{\partial B}{\partial x}\right|^n\left(\frac{\partial B}{\partial x}\right)B\right], \tag{1}$$

where $n=U_0/kT$ and $v_0=u\omega_m$. v_0 is the attempt velocity of the thermal-activated vortex motion, *u* is the hopping distance, and ω_m is the microscopic attempt frequency.

B. Boundary and initial conditions

In the *V-I* curve measurement, the current is always applied with a certain sweeping rate dI/dt. The boundary condition of Eq. (1) can be obtained from the current conservation equation: $(\partial/\partial t)\int_0^w\int_0^d j\,dx\,dz=dI/dt$. Substituting $\partial B/\partial x=-\mu_0 j$ into it, one obtains $B(d,t)-B(0,t)=-\mu_0 I/w$. Due to antisymmetry, one has $B(d,t)=-B(0,t)$, thus the boundary condition is

$$B(0,t)=\frac{\mu_0 I}{2w}=\left(\frac{\mu_0}{2w}\frac{dI}{dt}\right)t. \tag{2}$$

As for the initial condition, there is no current at $t=0$ in the sample, hence

$$B(x,0)=0. \tag{3}$$

C. Numerical method and the choice of parameters

Such kind of nonlinear diffusion equation can be numerically solved with the finite difference method. First, the temporal and spatial variances are discretized with different steps, respectively. Since the temporal and spatial steps are very important for the stability of the calculation, we take pains to choose suitable steps to avoid a divergence problem. Second, the equation is discretized and rewritten in an implicit difference scheme, which is better than the explicit difference scheme in the stability of calculation. Finally, based on the initial condition, the calculation by iteration will obtain the temporal and spatial magnitude of physical quantity, namely $B(x,t)$, $j(x,t)$, and $E(x,t)$. The voltage can be obtained by integration of $E(x,t)$. Note that the boundary condition plays a role of constraint in every time step during current ascending and descending, see Eq. (2).

It is easy to see that $U(j)=U_0\ln|j_c/j|$ combined with $E=E_0\exp(-U/kT)$ leads to the power dependence of the E-j curve $E=E_0(j/j_c)^n$ with $n=U_0/kT$. This power-law E-j curves are observed frequently in transport measurements and can be used to determine the parameter n.[15] Certainly, n is dependent on flux pinning strength, magnetic field, and temperature.[18,27] The weaker flux pinning and higher temperature bring about smaller n. In fact, many experiments including the present work show that for the Ag-Bi2223 in liquid-nitrogen temperature, $n=6$ is a typical value.

As for the velocity of the thermal-activated vortex motion and the critical current density, typical and reasonable magnitudes were employed based on the earlier theoretical and experimental work, for example we took $v_0=u\omega_m=1$ m/s (if $u\sim10^{-6}$ m, $\omega_m\sim10^6$ s^{-1}) and $j_{cW}=2\times10^8$ A/m^2. It should be pointed out that our numerical result is not sensitive to the choice of n, v_0, and j_{cW}.

D. Numerical results and discussions

1. Effect of j_{cS}/j_{cW} ratio on the hysteresis loop

Since j_c represents the pinning strength, the ratio j_{cS}/j_{cW} can be considered as a parameter reflecting the ratio of the two pinning strengths. Shown in Fig. 2 is our numerical result of the dependence of HE on j_{cS}/j_{cW} at fixed j_{cW}, d_S/d_W, and dI/dt. It is very clear that the V-I loop is clockwise as reported in Ref. 12. To understand how j_{cS}/j_{cW} affects the V-I loop, the corresponding current distributions in the sample were also calculated.

Note that the velocity of flux diffusion, namely the velocity of current diffusion in transport measurements, can be written as: $v=v_0\exp(-U/kT)\propto(j/j_c)^n$ for logarithmic $U(j)$. Hence, for the same j, the larger the j_c, the smaller the v. Generally speaking, the average speed of current diffusion in the S region ($\overline{v_s}$) is smaller than that of the W region ($\overline{v_w}$). In our calculation, j_{cW} is fixed, i.e., $\overline{v_w}$ is fixed. By changing the j_{cS}/j_{cW} ratio, namely j_{cS}, we adjust $\overline{v_s}$ only.

For a large ratio ($j_{cS}/j_{cW}=10$), i.e., high inhomogeneity of flux pinning, $\overline{v_s}$ is small compared with $\overline{v_w}$. And in such a case, there is no enough time for current diffusion in response to both the ascending branch of the V-I curve [Fig. 2.1(b)] and the descending one [Fig. 2.1(c)]. Consequently, no obvious V-I loop can be detected [Fig. 2.1(a)].

For a medium ratio ($j_{cS}/j_{cW}=4$), i.e., a medium inhomogeneity of flux pinning and a larger $\overline{v_s}$, it is shown that the area of the loop is very large [Fig. 2.2(a)]. In this case, although current has already penetrated into the S region during the ascending branch [Fig. 2.2(b)], much more current penetrates into S during the descending branch [Fig. 2.2(c)]. That is to say, the current diffusion of the S region has more time in response to the descending branch than to the ascending one. As a result, the V-I loop is obvious.

For a small j_{cS}/j_{cW} ratio, low inhomogeneity of flux pinning, $\overline{v_s}$ is very large and approaches $\overline{v_w}$. And there is little difference between the distributions of current during the two branches [Figs. 2.3(b) and (c)]. The minor difference is only seen when the current is small and the corresponding voltage is too small to be detected. Hence there is almost no hysteresis loop [Fig. 2.3(a)]. Especially at the uniform case ($j_{cS}/j_{cW}=1$, $\overline{v_s}=\overline{v_w}$), there will be no loop at all.

2. Effect of d_S/d_W ratio on the hysteresis loop

With a fixed total thickness, the spatial distribution of the S and W regions, i.e., the thickness ratio of them is also important for the V-I loop. The numerical V-I loops with different d_S/d_W at fixed dI/dt and j_{cS}/j_{cW} are displayed in Fig. 3. It is found that the smaller the d_S/d_W, the smaller the area of the loop.

For $d_S/d_W=0.857$ and other parameters given here, the thickness of the S region, i.e., the distance for current diffusion in the S region is so long that current diffusion in the S region has less time to respond to the ascending branch [Fig. 3.1(b)] than to respond to the descending one [Fig. 3.1(c)], so the area of the V-I loop is large [Fig. 3.1(a)].

For $d_S/d_W=0.222$, the S region is thinner, i.e., the distance of current diffusion in the S region is shorter, resulting that compared with the $d_S/d_W=0.857$ case, the current diffusion in the S region has more time in response to the ascending current [Fig. 3.2(b)]. In other words, for such parameters given here, the response time of current diffusion in the S region to the two branches of the V-I loop shows little difference. As a result, the area of the V-I loop becomes smaller [Fig. 3.2(a)].

As for $d_S/d_W=0.105$, the S region is too thin and the distance of current diffusion in the S region is too short. Hence there is enough time for current diffusion in response to both current ascending and descending at the given parameters [Figs. 3.2(b) and (c)]. That is to say, there is no obvious V-I loop [Fig. 3.3(a)]. As d_S/d_W approaches 0, namely the uniform flux pinning case, the hysteresis loop will disappear thoroughly.

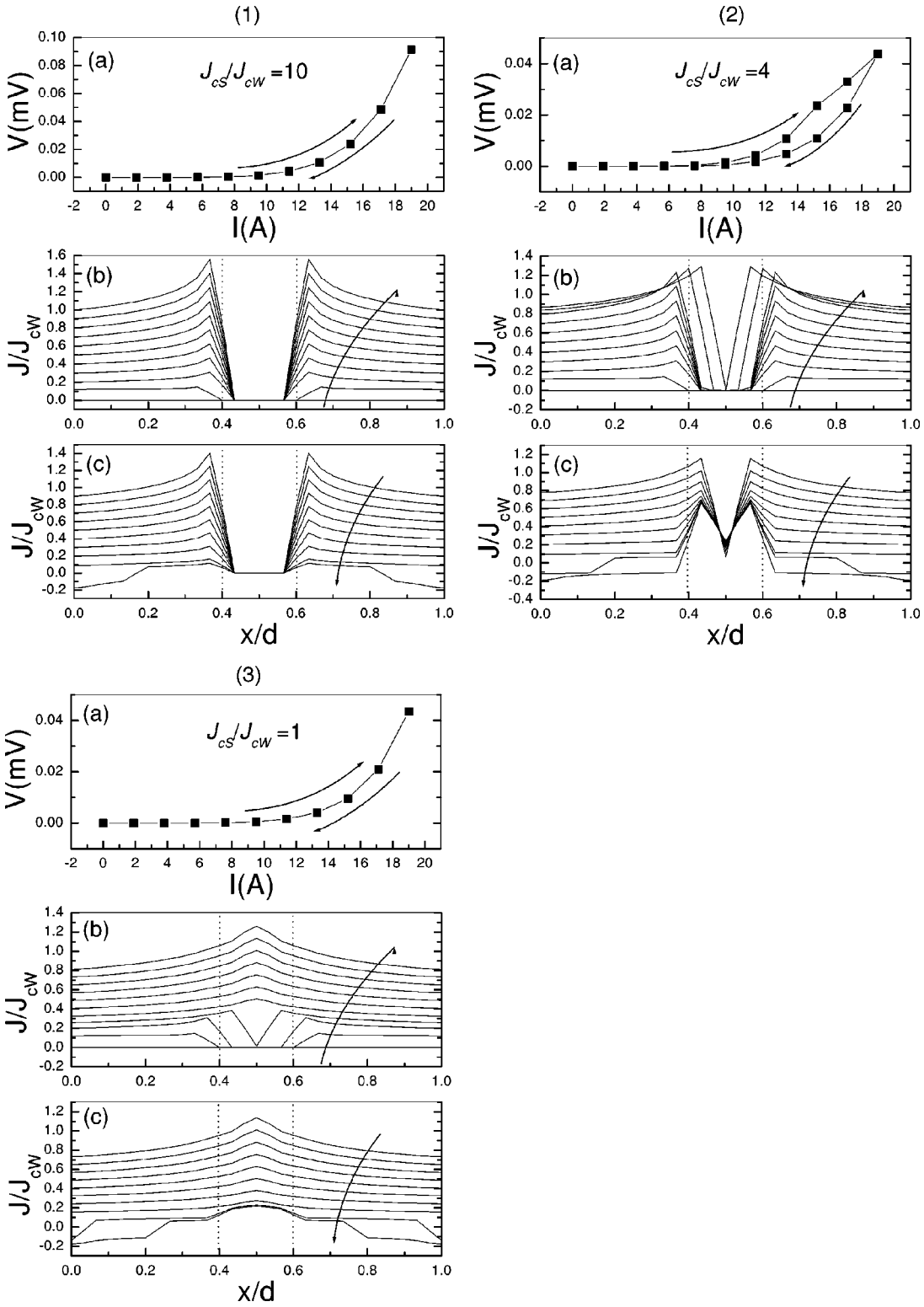

FIG. 2. Numerical results, showing the effect of j_{cS}/j_{cW} ratio on the *V-I* loop (a) and the distribution of current during the ascending (b) and descending branch (c) of the loop. The arrows indicate the increasing and decreasing of current, i.e., the time evolution. The dot lines represent the boundary between the *S* and *W* regions. $d_S/d_W=1/2$, $dI/dt=1$ A/s, $j_{cW}=2\times10^8$ A/m^2. (2.1) $j_{cS}/j_{cW}=10$, high inhomogeneity of flux pinning. Average speed of current diffusion in the *S* region is too small compared with that of the *W* region, so that in the *S* region there is not enough time for current diffusion in response to both the ascending sweeping and the descending one at the given parameters. There is no obvious *V-I* loop. (2.2) $j_{cS}/j_{cW}=4$, medium inhomogeneity of flux pinning and larger than average speed of current diffusion in the *S* region, so that more current has penetrated into the *S* region during the descending branch than the ascending one at the given parameters. An obvious *V-I* loop is observed. (2.3) $j_{cS}/j_{cW}=1$, uniform flux pinning, equal average speed of current diffusion in the two regions. There is little difference between the distributions of current during the two branches. There is no obvious *V-I* loop.

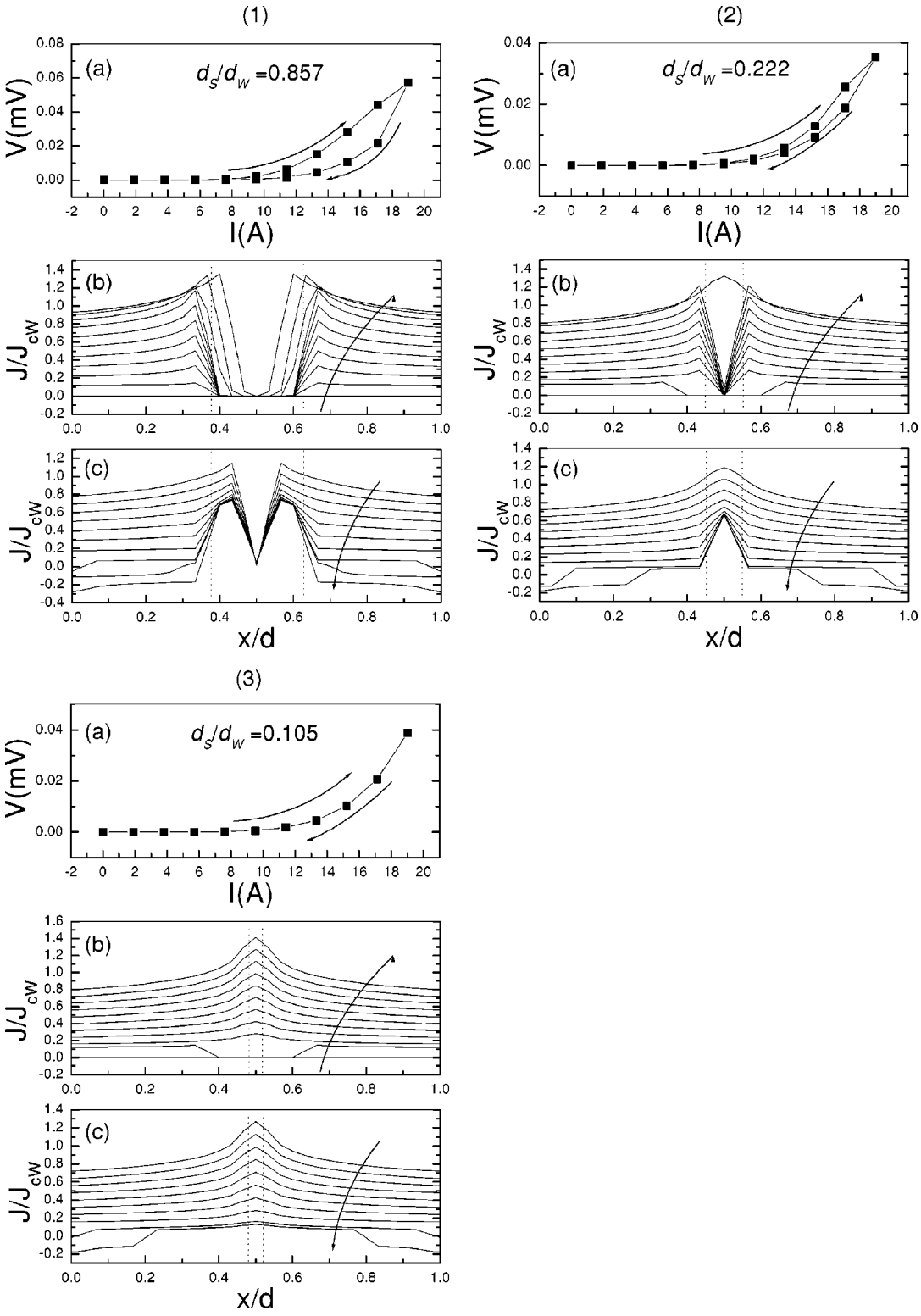

FIG. 3. Numerical results, showing the effect of d_S/d_W ratio on the *V-I* loop (a) and the distribution of current during the ascending (b) and descending branch (c) of the loop. $j_{cS}=4j_{cW}$, $dI/dt=1$ A/s, $j_{cW}=2\times10^8$ A/m^2. (3.1) $d_S/d_W=0.857$, the thickness of the *S* region is proper, so that in the *S* region there is enough time for current diffusion in response to current descending, but the current diffusion is too busy to respond to current ascending for the given parameters, and the area of the *V-I* loop is large. (3.2) $d_S/d_W=0.222$, the *S* region is thinner, and the distance of current diffusion in the *S* region is shorter, so that in the *S* region there is much more time for current diffusion in response to current ascending at the given parameters, and the area of the *V-I* loop becomes smaller. (3.3) $d_S/d_W=0.105$, the *S* region is too thin, and the distance of current diffusion in the *S* region is too short, so that in the *S* region there is enough time for current diffusion in response to both the current ascending and descending at the given parameters. There is no obvious *V-I* loop.

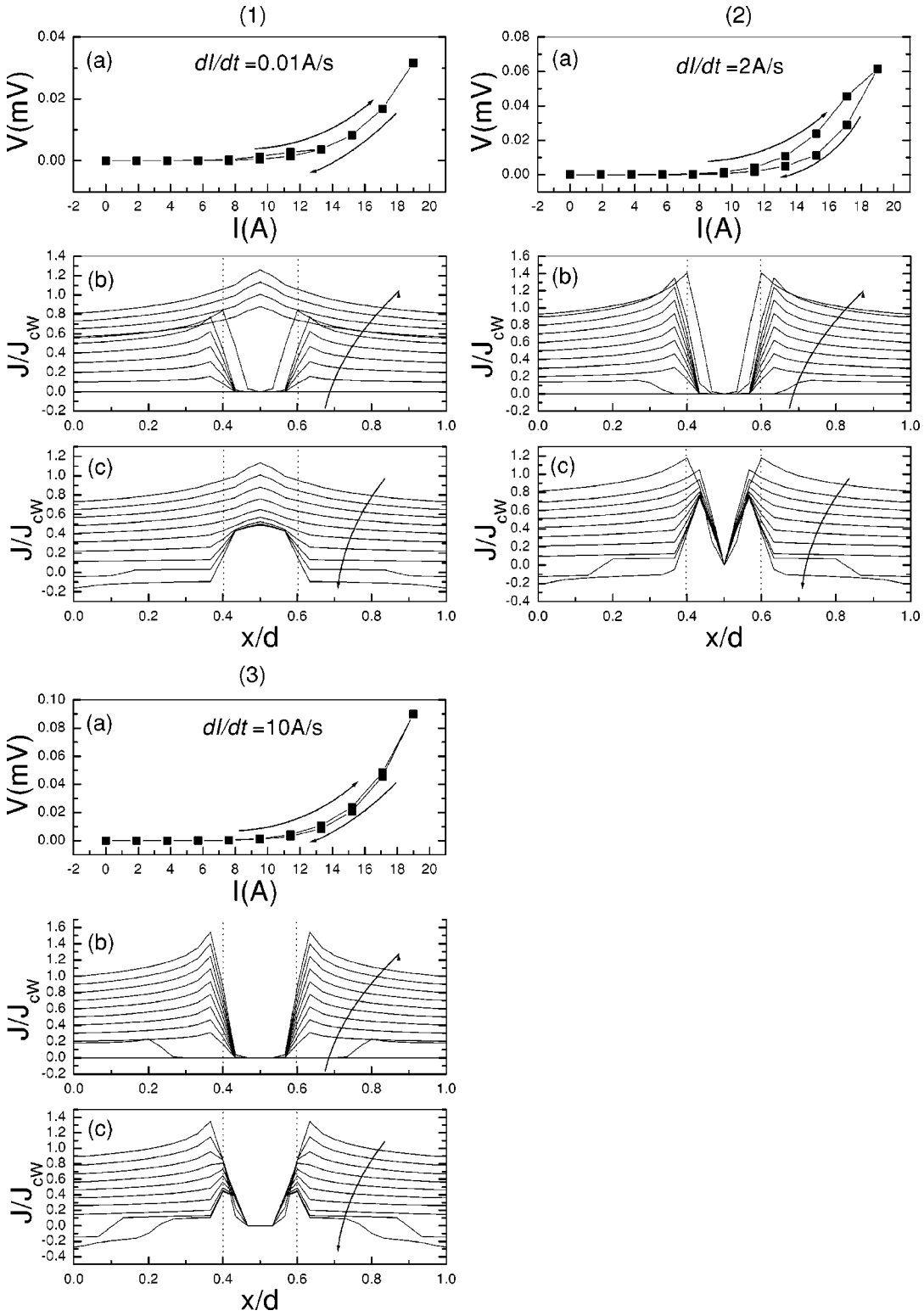

FIG. 4. Numerical results. Current sweeping rate dependent *V-I* loop (a). The corresponding distributions of current during the ascending (b) and descending branch (c) were also shown. $d_S/d_W=1/2$, $j_{cS}/j_{cW}=4$, $j_{cW}=2\times10^8$ A/m^2. (4.1) $dI/dt=0.01$ A/s, the current sweeping rate is so slow that in the *S* region there is enough time for current diffusion in response to both the ascending and descending current sweeping at the given parameters. There is no obvious *V-I* loop. (4.2) $dI/dt=2$ A/s, the current sweeping is faster, so that in the *S* region there is not enough time for current diffusion in response to current ascending at the given parameters, and the *V-I* loop is larger. (4.3) $dI/dt=10$ A/s, the current sweeping is so fast that in the *S* region there is not enough time for current diffusion in response to both the ascending and descending current sweeping at the given parameters. There is no obvious *V-I* loop.

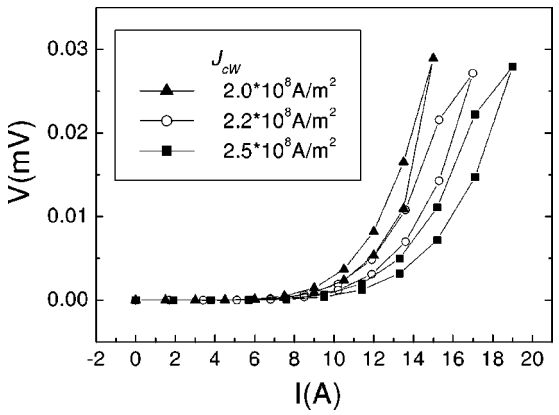

FIG. 5. Numerical results. Magnetic-field-dependent *V-I* loop, where the area of the loop is insensitive to j_{cW} while the transport j_c is strongly affected by magnetic field. $d_S/d_W=1/2$, $j_{cS}=8\times10^8$ A/m^2, $dI/dt=1$ A/s.

3. Current sweeping rate (dI/dt) *dependent V-I loop*

The numerical result of current sweeping rate dependent *V-I* loops at fixed j_{cS}/j_{cW} and d_S/d_W is illustrated in Fig. 4.

It is seen that if dI/dt is very small, such as 0.01 A/s, flux lines will have enough time to respond the changing applied current and thus can penetrate into both *W* and *S* regions. The difference of current distribution during the ascending [Fig. 4.1(b)] and descending branch [Fig. 4.1(c)] is very small. As a result, the area of the *V-I* loop is also small [Fig. 4.1(a)]. As dI/dt reaches a moderate value, say $dI/dt=2$ A/s, the difference between the current distributions during the ascending and descending branch is larger, and the area of the *V-I* loop becomes larger too [Fig. 4.2(a)]. Nevertheless, when dI/dt is too large, say $dI/dt=10$ A/s, the area of the *V-I* loop decreases dramatically [Fig. 4.3(a)]. It is easy to understand that in such a case, compared with dI/dt, v_s is so small that the current cannot penetrate into the *S* region during both the ascending and descending branch, and the corresponding current distributions during the two branches do not show a visible difference [Figs. 4.3(b) and (c)]. So there is no obvious *V-I* loop.

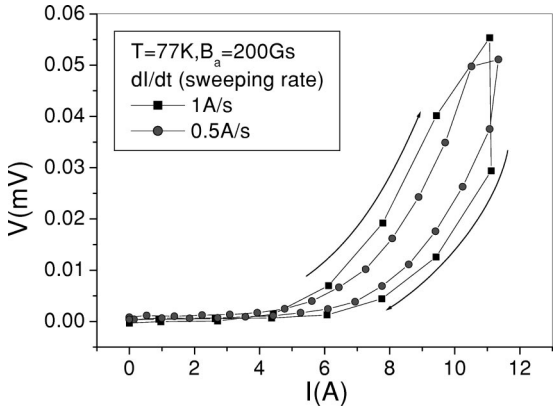

FIG. 6. Experimental *V-I* loops of the Ag-Bi2223 tape with different current sweeping rates dI/dt, which is qualitatively with the numerical curves shown in Fig. 4 and is a conformation of our model.

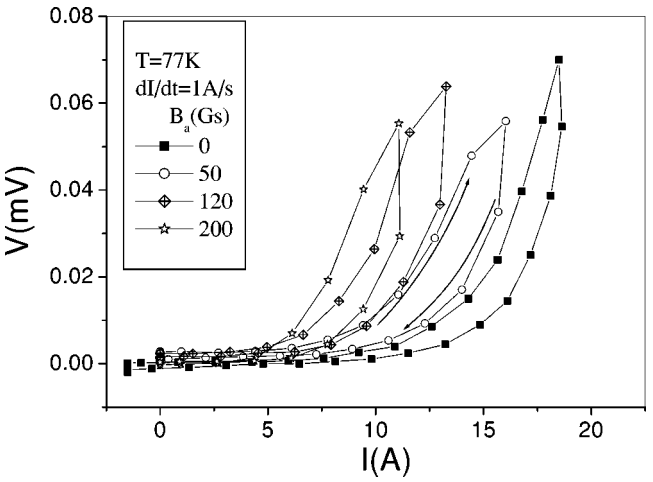

FIG. 7. Experimental *V-I* loops of the Ag-Bi2223 tape at different applied magnetic fields, which is qualitatively with the numerical curves shown in Fig. 5. It is noted that the area of the loop is insensitive to B_a whereas the value of the j_c is strongly affected by magnetic field, which supports the present model further.

Now, it is clear what the effect of dI/dt on the *V-I* loop means. With fixed distance and average speed of the current diffusion, to change dI/dt is equivalent to shift our observing time window. When we choose the time window by using dI/dt as 10 A/s, the observing time is so early that there is not enough current inside the *S* region by means of diffusion even when the applied current sweeping has been finished. Of course there is no detectable *V-I* loop. If we use $dI/dt=0.01$ A/s, we shift our time window so late that there is always enough current diffused into the *S* region during both the ascending and descending branches. It is natural that no obvious *V-I* loop exists at all. Only when we choose a proper observing window, i.e., a proper dI/dt such as 2 A/s, is there much more current in the *S* region during the descending branch than the ascending one. In other words, only in such a case can the current diffusion in the *S* region have more time to respond to the descending branch than the ascending one, and the *V-I* loop will be obvious.

In conclusion, if there is more time for current diffusion of the *S* region to respond to the descending branch than to respond to the ascending one, the hysteresis loop in the *V-I* curve, i.e., the HE, will be obvious. On the other hand, if the current diffusion time of the *S* region is similar or the same for the ascending and descending branches, there will be no obvious *V-I* loop, namely no HE. The observation of HE can be controlled by adjusting dI/dt (the observing time window) or d_S/d_W (the distance of current diffusion) or j_{cS}/j_{cW} (the average speed of current diffusion).

4. Magnetic-field-dependent V-I loop

It is well known that j_c is dependent on the magnetic field B_a. Commonly, j_c decreases with increasing B_a. Therefore studying the effect of j_c on the *V-I* loop is equivalent to studying the effect of B_a on it. For the inhomogeneous pinning case, j_{cW} is more sensitive to B_a than j_{cS}, especially when B_a is not very high.[19] Thus we simulated the *V-I* loops

in different applied fields B_a, namely different j_{cW} at fixed j_{cS}, dI/dt, and d_S/d_W. Shown in Fig. 5 are the numerical results. It is clearly seen that the loop shifts towards smaller current with decreasing j_{cW} while the area of the loop is insensitive to j_{cW}. In other words, the area of the loop is weakly affected by magnetic field.

As mentioned above, the existence of HE depends on the current diffusion of the *S* region having different responding times for the two sweeping branches of the *V-I* loop. Only changing j_{cW}, i.e., B_a, would not affect the responding time of the *S* region. As a result, the area of the *V-I* loop will not change acutely.

IV. EXPERIMENT

Because our numerical simulation has obtained more results than the experimental one reported in Ref. 12, such as the effect of dI/dt on the area of loops, we measured *V-I* curves of Ag-Bi2223 samples in various applied magnetic fields B_a with different dI/dt to confirm the numerical prediction. It has been pointed out above that the Ag-Bi2223 sample may be proper to test our model.

The Ag-Bi2223 samples cut from long silver sheathed tapes come from the National Center for R&D on Superconductivity of China. All the samples are *c*-axis textured. The *c* axis is perpendicular to the wider surfaces of the samples. Including the outer silver sheath, the average size of the samples is approximately 4 mm$\times$1 mm$\times$4 cm. Between each two neighbor points of four (two voltage contacts and two current contacts) is 1 cm in length. The transport measurement was carried out for the sample immersed in liquid nitrogen. The external magnetic field with range 0–200 Gs was applied in the superconducting state. The current range of the supply source is 0–40 A and the sweeping rate range is 0.02–1 A/s. The measurements were made in the case of B_a parallel to the *c* axis of the samples. More details of the sample preparation and the measurements can be found in Ref. 18.

The *V-I* loops were measured by ascending current first and then descending it. Displayed in Fig. 6 are the experimental *V-I* loops with different dI/dt and fixed B_a. The spottiness of the experimental data came from the limited picking rate of our measurement system. As reported in Ref. 12, a clockwise loop of *V-I* curve was observed. It is clearly seen that dI/dt affected not only the appearance of the *V-I* curve but also the area of the loop. For example, the area of loop with $dI/dt=1$ A/s is larger than the area of loop with $dI/dt=0.5$ A/s, which is in good agreement with the numerical result.

Shown in Fig. 7 are the experimental *V-I* loops in different applied fields B_a at a fixed dI/dt. It is found that the area of the loop is insensitive to magnetic field B_a whereas the transport critical current density j_c decreases with increasing applied field very sensitively. This experimental dependence confirms the above numerical results and thus supports strongly our model. Furthermore, the agreement between the numerical and experimental *V-I* shifting by applied field implies that the critical current density j_c of a sample with spatially nonuniform flux pinning strength, such as the silver sheathed Bi2223 tapes, is governed mainly by the weaker flux pinning region (the region with smaller j_c). Hence for these HTS materials, which have potential for technical applications, the point to enhance their critical current density is to improve the flux pinning strength of weak pinning region.

We are unable to measure more *V-I* curves to test all the numerical curves for the limited ability of our instrument. For example, dI/dt cannot be too small because Ohm heat at the current contacts will destroy the sample.

V. SUMMARY

We have proposed a model to account for a different kind of history effect in an inhomogeneous flux pinning superconductor at high temperatures. The model consists of alternating weak and strong flux pinning regions whose strength was depicted by different critical current densities j_{cW} and j_{cS}, respectively. Based on the model, our numerical simulation successfully observed a hysteresis loop in the characteristic *V-I* curve as reported in references. Our numerical results also predicted some interesting characteristics of the *V-I* loop at different sweeping rates of applied current dI/dt, applied magnetic fields B_a, the ratio of the two regions' pinning strength, and their thickness.

Physically, due to the difference of flux pinning strength in the *S* and *W* regions, the average speeds of flux (or current) diffusion in the two regions are different too. If dI/dt (or d_S/d_W, j_{cS}/j_{cW}) is proper, the *V-I* loop, i.e., the HE, is obvious. Otherwise, no obvious *V-I* loop can be observed.

To confirm the numerical results, electric transport measurement was conducted to get the characteristic *V-I* curve of Ag-sheathed $Bi_{2-x}Pb_xSr_2Ca_2Cu_3O_y$ tapes immersed in liquid nitrogen with or without applied fields. A clockwise *V-I* loop was observed to be dependent on dI/dt and B_a. Hence we presented a possible mechanism accounting for a different kind of HE in an inhomogeneous flux pinning superconductor.

ACKNOWLEDGMENTS

The work was supported by the Ministry of Science and Technology of China (NKBRSF-G1999-0646) and NNSFC (No.19994016). Numerical simulations were done on the SGI Origin 3800 of Nanjing University.

*Corresponding author. Email address: syding@netra.nju.edu.cn

[1] W. Henderson, E.Y. Andrei, M.J. Higgins, and S. Bhattacharya, Phys. Rev. Lett. **77**, 2077 (1996); Z.L. Xiao, E.Y. Andrei, P. Shuk, and M. Greenblatt, *ibid.* **85**, 3265 (2000).

[2] Y. Paltiel, E. Zeldov, Y.N. Myasoedov, H. Shtrikman, S. Bhattacharya, M.J. Higgins, Z.L. Xiao, E.Y. Andrei, P.L. Gammel, and D.J. Bishop, Nature (London) **403**, 398 (2000).

[3] S. Kokkaliaris, P.A.J. de Groot, S.N. Gordeev, A.A. Zhukov, R. Gagnon, and L. Taillefer, Phys. Rev. Lett. **82**, 5116 (1999).

[4] S. Bhattacharya and M.J. Higgins, Phys. Rev. B **52**, 64 (1995).

[5] S.O. Valenzuela and V. Bekeris, Phys. Rev. Lett. **84**, 4200 (2000).
[6] S.S. Banerjee, N.G. Patil, S. Saha, S. Ramakrishnan, A.K. Grover, S. Bhattacharya, G. Ravikumar, P.K. Mishra, T.V. Chandrasekhar Rao, V.C. Sahni, M.J. Higgins, E. Yamamoto, Y. Haga, M. Hedo, Y. Inada, and Y. Onuki, Phys. Rev. B **58**, 995 (1999).
[7] R. Wördenweber, P.H. Kes, and C.C. Tsuei, Phys. Rev. B **33**, 3172 (1986).
[8] S.S. Banerjee, N.G. Patil, S. Ramakrishnan, A.K. Grover, S. Bhattacharya, P.K. Mishra, G. Ravikumar, T.V. Chandrasekhar Rao, V.C. Sahni, M.J. Higgins, C.V. Tomy, G. Balakrishnan, and D. Mck. Paul, Phys. Rev. B **59**, 6043 (1999).
[9] S.S. Banerjee, S. Ramakrishnan, A.K. Grover, G. Ravikumar, P.K. Mishra, V.C. Sahni, C.V. Tomy, G. Balakrishnan, D. Mck. Paul, P.L. Gammel, D.J. Bishop, E. Bucher, M.J. Higgins, and S. Bhattacharya, Phys. Rev. B **62**, 11 838 (2000).
[10] A.A. Zhukov, S. Kokkaliaris, P.A.J. de Groot, M.J. Higgins, S. Bhattacharya, R. Gagnon, and L. Taillefer, Phys. Rev. B **61**, R886 (2000).
[11] H. Safar, P.L. Gammel, D.A. Huse, D.J. Bishop, J.P. Rice, and D.M. Gingsberg, Phys. Rev. Lett. **69**, 824 (1992).
[12] P. Ušák, L. Janšák, and M. Polák, Physica C **350**, 139 (2001).
[13] A.I. Larkin and Y.N. Ovchinnikov, J. Low Temp. Phys. **34**, 409 (1979).
[14] L.P. Ma, C.H. Li, R.L. Wang, and L. Li, Physica C **279**, 143 (1997).
[15] S.Y. Ding, C. Ren, X.X. Yao, Y. Sun, and H. Zhang, Cryogenics **38**, 809 (1998).
[16] P. Zhang, C. Ren, S.Y. Ding, Q. Ding, F.Y. Lin, Y.H. Zhang, H. Luo, and X.X. Yao, Supercond. Sci. Technol. **12**, 571 (1999).
[17] S.Y. Ding, H. Luo, Y.H. Zhang, Q. Ding, F.Y. Ling, P. Zhang, X.F. Wu, L. Qiu, and X.X. Yao, J. Supercond. **40**, 29 (2000).
[18] Y.H. Zhang, H. Luo, X.F. Wu, and S.Y. Ding, Supercond. Sci. Technol. **14**, 346 (1999).
[19] Ph. Vanderbemden, R. Cloots, M. Ausloos, R.A. Doyle, A.D. Bradley, W. Lo, D.A. Cardwell, and A.M. Campbell, IEEE Trans. Appl. Supercond. **9**, 2308 (1999).
[20] R. Wördenweber, Rep. Prog. Phys. **62**, 187 (1999).
[21] D.S. Fisher, M.P.A. Fisher, and D.A. Huse, Phys. Rev. B **43**, 130 (1991).
[22] M.V. Feigel'man, V.B. Geshkenbein, A.I. Larkin, and V.M. Vinokur, Phys. Rev. Lett. **63**, 2303 (1989).
[23] J. Mannhart and C.C. Tsuei, Z. Phys. B: Condens. Matter **77**, 53 (1989).
[24] H. Ullmaier, *Irreversible Properties of Type II Superconductors* (Springer-Verlag, Berlin, 1975), pp. 89–94.
[25] G. Blatter, M.V. Feigel'man, V.B. Geshkenbein, A.I. Larkin, and V.M. Vinokur, Rev. Mod. Phys. **66**, 1125 (1994).
[26] V.M. Vinokur, M.V. Feigel'man, and V.B. Geshkenbein, Phys. Rev. Lett. **67**, 915 (1991).
[27] Y.H. Zhang, Z.H. Wang, H. Luo, X.F. Wu, H.M. Luo, and S.Y. Ding, J. Phys.: Condens. Matter **13**, 2583 (2001).